第 24 回日本バーチャルリアリティ学会大会論文集（2019 年 9 月）

# Design of Freeform Lens for Portable Mid-air Imaging System

Design of Freeform Lens for Portable Mid-Air Imaging System

金四維 [1)]，横瀬哲也 [2)]，阪口紗季 [3)]，苗村健 [1,2,3)]
Siwei JIN, Tetsuya YOKOSE, Saki SAKAGUCHI, and Takeshi NAEMURA

1) 東京大学大学院 情報理工学系研究科 （〒113-8656 東京都文京区本郷 7-3-1,{jin, naemura}@nae-lab.org）
2) 東京大学大学院 学際情報学府 （〒113-0033 東京都文京区本郷 7-3-1, yokose@nae-lab.org）
3) 東京大学大学院 情報学環 （〒113-0033 東京都文京区本郷 7-3-1, sakaguchi@nae-lab.org）

Abstract：We present a structure of adding freeform lens in the mid-air imaging system made from RT-Plate to increase the portability of the system. The result of simulation shows the proposed system will be thinner than the traditional system.

Keyword：Mid-air display; Optics; Freeform lens; Mid-air image

## 1. Introduction

Mid-air images are often described in fiction movies but not yet used in daily life. Many types of 3D mid-air imaging system are developed. Optical imaging elements[1], fog screen[2] or plasma emission[3] are used for displaying in mid-air. Most of them are based on volumetric displaying method that generate 2D mid-air image by imaging elements and move it by a scanner[4], where the 3D image is a sequence of 2D image.

2D mid-air image is generated with many different methods, like retro-reflection[5] or mirror reflection[6,7]. Retro-transmissive plate(RT-Plate) is one of them. It is made of two layers of micro mirror arrays. This arrangement makes all light emitted from light source focus on the symmetric point about the plane of RT-Plate, which also means the size of the optical system with RT-Plate should be nearly the same as the distance of image popping out from RT-Plate that you want. On the other hand, this arrangement also brings limit to angle of view. The angle of view is restricted near $45^{o}$ to have the best quality of mid-air image.

Freeform Lens(FFL) is a new type of lens that greatly different from traditional symmetric lens. Traditional lenses have at least one symmetric axis, which is usually a rotational symmetric axis, but the FFLs can be designed to be arbitrary shape without symmetric axis. Of course it requires more precision of processing and the technique nowadays can meet the needs of the manufacture.

FFL become popular in recent years as manufacturing technology developed and the flexibility in designing from extra degrees of freedom. The extra degrees of freedom make FFL has more function in certain space, but is still restricted in some extent. Although FFL is used in non-imaging optics at first[8,9], it is used in imaging optics, such as head-mounted displays[10,11], reflective systems[12] and panoramic lens[13].

With only RT-Plate, it should be placed away from the display as far as the mid-air image popping out from the RT-Plate you want, and the angle is restricted to near 45 degrees to keep the best image quality, as shown in Fig.1. We cannot compress the light path, keep the best quality and popping the mid-air image out far enough at the same time.

This paper designed a FFL adding in this mid-air imaging system to compress the light path and improve the portability of the system, and keeping the best image quality as well as shown in Fig.2 that the FFL generates a virtual image of the display behind the it with a certain angle $\alpha$ that is less than 45 degrees, which compress the distance between RT-Plate and display, increase the pop out distance of the aerial image and hold the best angle of view at the same time.

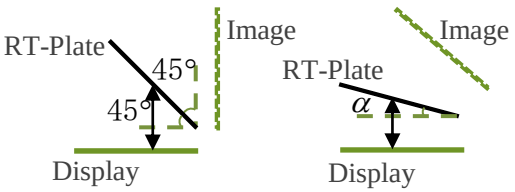


Fig.1 Layout of the fields and the change of overlap area of the neighboring fields while the angle of FOV increased

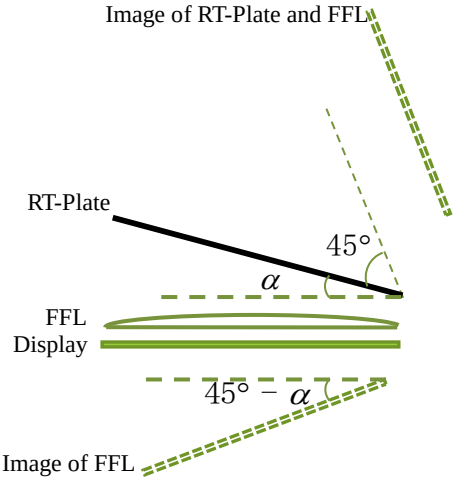


Fig.2 Adding FFL between RT-Plate and display

## 2. Surface contour method

Surface contour method is used to design FFL in this paper. With this method we can design lens with wide field of view(FOV)[14]. The core of surface contour method is dividing the FOV ($\pm\ \omega$) into 2k+1 fields with fixed intervals of angle with fixed interval $\Delta\omega$ between each two neighboring fields, where $\Delta\omega$ can be expressed as

$$\Delta\omega = \frac{\omega}{k}$$

Different situation happens as angle of FOV changes and different process is made to calculate the data point.

Neighboring fields generate overlap areas when the angle of FOV is small. The overlap area gets smaller as the angle of FOV increased and disappear after certain angle, as shown in Fig. 3. The number of light rays that used to calculate the data point changes whether there are overlap areas or not, as shown in Fig. 4. We need 2 feature rays to calculate the data point 2 in the overlap area in Fig. 4(a) but only 1 feature ray to calculate the data point out of the overlap area in Fig. 4(b).

The data points on the front surface can be calculated by the incident and the refracted rays in field groups of each two

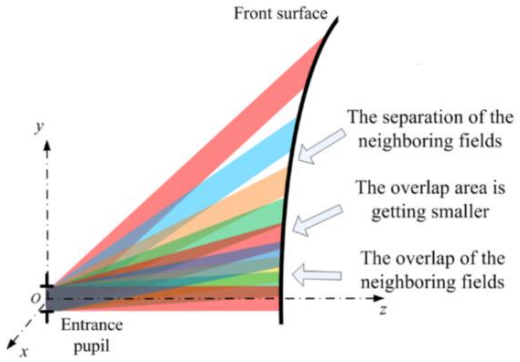


Fig.3 Layout of the fields and the change of overlap area of the neighboring fields while the angle of FOV increased

neighboring fields. Geometric relations between the neighboring field groups that the normal vector at the one data point is perpendicular to the line between this data point and the previous data point should be added to constrain data points. The stairs-distribution elimination constraint should be added to avoid the stair distribution of the data points shown in Fig. 5, which is hard to fit data points to a smooth surface contour. The stairs-distribution elimination constraint is shown in Fig. 6 that the intersection point of lines that connecting two data points in neighboring groups $P_i$ should be between the two neighboring points of two groups. That is

$$(P_{2y} - P_{iy})(P_{3y} - P_{iy}) < 0$$
$$(P_{2z} - P_{iz})(P_{3z} - P_{iz}) < 0$$

The stair distribution can be eliminated and smooth link line between data points can be generated.

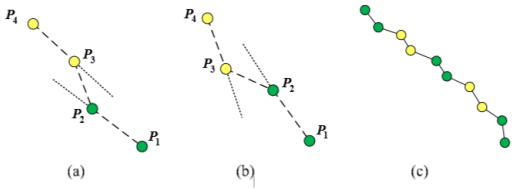


Fig. 5 Examples of the stair distributions of the data

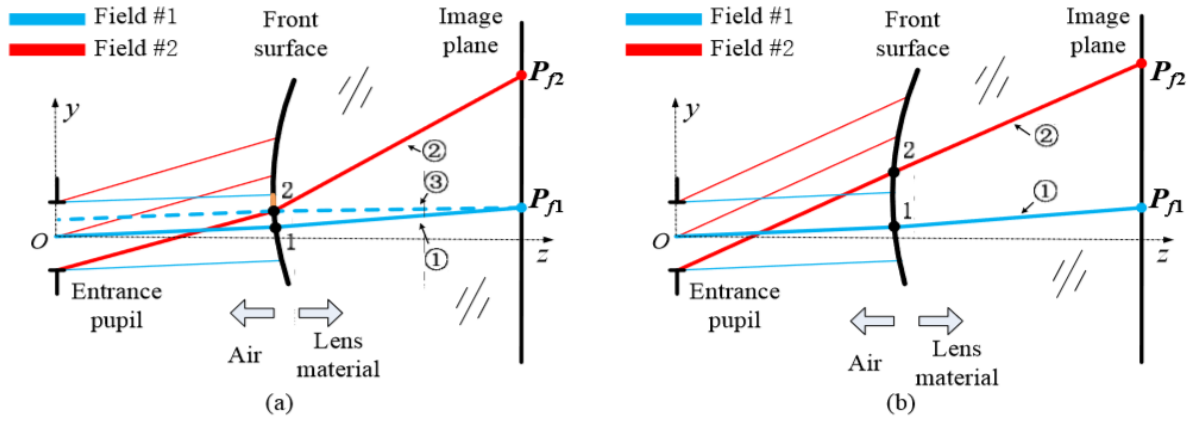


Fig. 4 The definition of the feature rays used in each field group to calculate the data points on the freeform surface. (a) When the two neighboring fields have overlap area on the unknown surface. (b) When the light beams are separated.

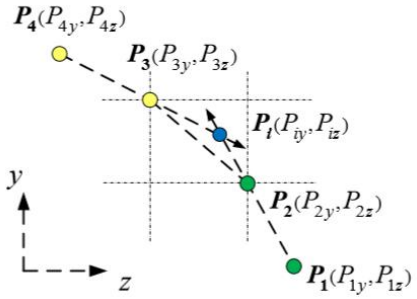


Fig. 6 The stair-distribution elimination constraint

## 3. Simulation and experiment

### 3.1 Simulation

The layout is shown in Fig.7. The angle of display and image plane is 30 degrees. Light rays starts from the display and reach the rear surface of the FFL to refractive first time, and then refractive at the front surface of FFL for the second time. Light rays will be divergent as if it was emitted from the virtual image of display. D, H and L are three parameters that will be changed according to the design. The model of display (light source) is iPhone 8, therefore the size of it is 13.84cm*6.73cm. To cover more emit light rays, the size of FFL is set to be a little bit bigger than display and finally we make it to 15cm*8cm. The material for FFL is set to be PMMA whose refractive index is nearly 1.49. The rest part of the layout is filled with air whose refractive index is 1.00.

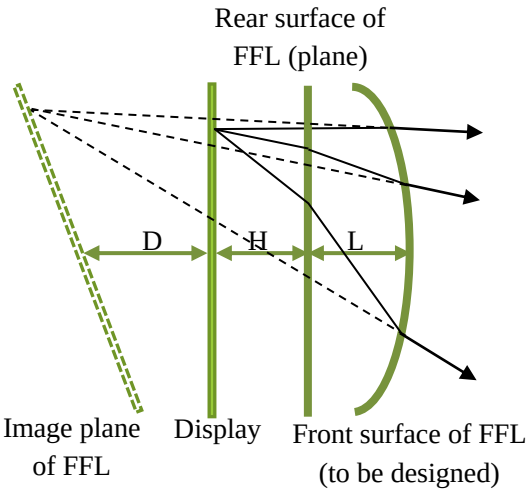


Fig. 7 Layout of Simulation

As surface contour method was developed on a 2D plane, we can only get a profile of the FFL. There are two ways to construct the whole freeform surface. The 1st way is to calculate two baselines on two directions by surface contour method and interpolate the rest part of the surface, as shown in Fig.8(a), and the 2nd way is calculating all rows (or columns) with the start point on the same baseline calculated by surface contour method, as shown in Fig.8(b).

The calculating of data points and surface construction are done by MATLAB and simulation is done by the Zemax.

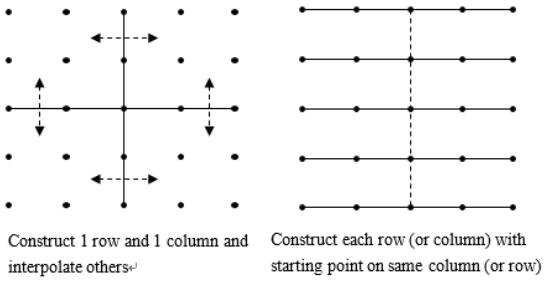


Fig. 8(a)1st construction way (b) 2nd construction way

### 3.2 Experiment

We used 3D printer to print the prototype of our design. Material is the clear resin whose refractive index is around 1.5. A smaller one with size 1:10 of the design is printed for experiment. Although all the sanding and polishing procedure follows the instruction on official website of the 3D printer about how to print a lens with clear resin, all of the procedure is done by ourselves so the precision is restricted.

## 4. Result

The design is based on the initial parameter D=H=L=10cm, and the simulation result on the image plane with initial parameter of two surface construction methods is shown in Fig.9. However both of them has distortion of being a trapezoid and the chromatic aberration, it can be easily found out from the figure that the result of the 1st way is worse than the result of 2nd way with more blurry at the bottom. Following simulation will be conducted by 2nd way.

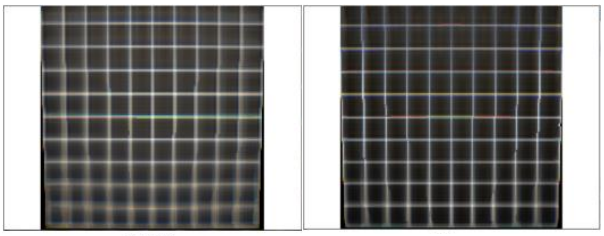

1st way 2nd way

Fig.9 Result of two surface construction method with initial parameter

The result of a few variations of the parameter triplets are shown in Fig.10. While D=H=L=10cm still holds the best quality of image in all variations.

The result of the experiment is shown in Fig.11. The arrangement of experiment is the same with the simulation layout but in 1:10 size, which is H=1cm. There is unexpected distortion in the upper part of the image. It seems like the trapezoid distortion showed in the simulation but the direction changes. And the result of the simulation shows that the middle of the image should have the best quality but the experiment did not. The reason is thought to be the bad technique in sanding

that may have done harm to the optical surface of the lens.

Another problem of the experiment is that the lens seems to be like a frosted glass. We can't see through the lens very clearly even though all the sanding and polishing procedure from the official website is finished.

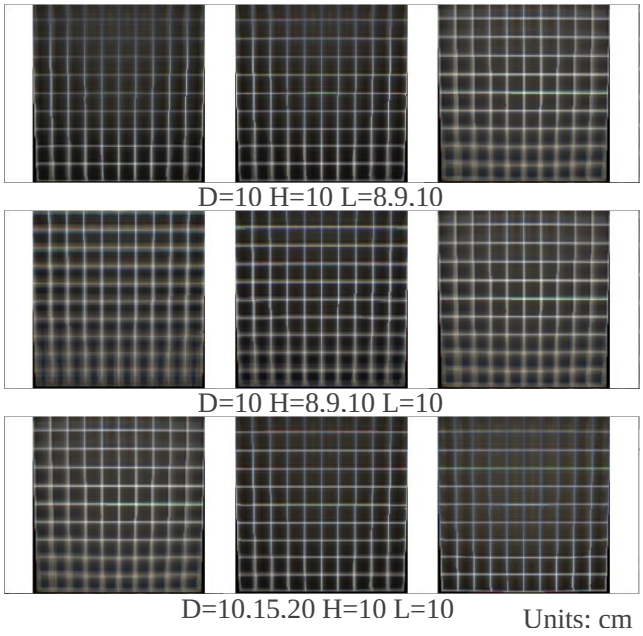


Fig.10 Result of simulation with various of parameter

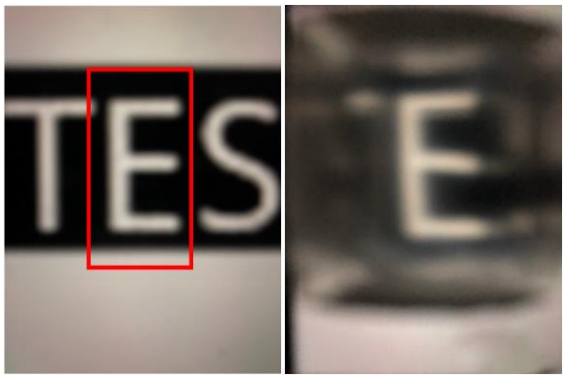


Fig.11 Result of experiment

## 5. Conclusion

It is shown from the result that the FFL has succeeded in generating a virtual image behind the display and changing the direction of the virtual image plane according to the result of simulation. But the quality of the image is not acceptable and the best parameter triplets will lead the thickness of the whole system to 20cm, not matching the portability of smart phones. A lens with the thickness of 10cm will not be acceptable for its weight to be as portable as a smart phone, either.

We will aim at reducing the scale of the mid-air imaging system and the target is reducing thickness to less than 10cm while keeping nearly the same distance between aerial image and display.

## Reference

[1] Q. Smithwick, L. S. Smoot, and D. Reetz, "A volumetric display using arim-driven varifocal beamsplitter and high-speed DLPbacklit LCD". SID Symp. Dig. Tech. Papers 43, 792–795 (2012).

[2] V. Vasilevskiy, "Method and device for forming an aerosol projection screen," patent WO2014046566 A1 (2012).

[3] H. Ishikawa, H. Watanabe, S. Aoki, H. Saito, S. Shimada, M. Kakehata, Y. Tsukada, and H. Kimura, "Surface representation of 3D objects for aerial 3D display," Proc. SPIE 7863, 78630X (2011).

[4] Y. Maeda, D. Miyazaki, and T. Mukai, "Magnifying a three dimensional image displayed by a volumetric display based on optical scanning of an inclined image plane," in Proceedings of the International Display Workshops '13 (2013), pp. 1090–1093.

[5] H. Yamamoto and S. Suyama, Aerial imaging by retro-reflection (AIRR). SID Symposium Digest of Technical Papers. (2013)

[6] S. Maekawa, K. Nitta, and O. Matoba, "Transmissive optical imaging device with micromirror array," Proc. SPIE 6392, 63920E (2006).

[7] ASUKANET. Aerial imaging plate. In Japanese patent No.P5437436 (2013).

[8] F. Munoz, et al., High-order aspherics: The SMS non-imaging design method applied to imaging optics. (2008).

[9] K. Lin, "Freeform Lens Design for Illumination with Different Luminance Intensities". J Comput Sci Syst Biol (2015)

[10] Q. Wang, et al., "Design, tolerance, and fabrication of an optical see-through head-mounted display with free-form surface elements," Appl. Opt. 52, C88-C99 (2013)

[11] S. Steven, et al., "Augmented reality display system for smart glasses with streamlined form factor," Proc. SPIE 10676, Digital Optics for Immersive Displays, 106761I (2018)

[12] J. C. Papa, J. M. Howard, J. P. Rolland, "Three-mirror freeform imagers," Proc. SPIE 10690, Optical Design and Engineering VII, 106901D(2018)

[13] T. Ma, J. Yu, P. Liang, and C. Wang, "Design of a freeform varifocal panoramic optical system with specified annular center of field of view," Opt. Express 19, 3843-3853 (2011)

[14] J. Zhu, T. Yang, and G. Jin, "Design method of surface contour for a freeform lens with wide linear field-of-view," Opt. Express 21, 26080-26092 (2013)